

Thermodynamic, Transport, and Excitation Properties of Ce Impurities in a Model Metal: Kondo Resonance and Universality in the Mixed-Valent Regime

N. E. Bickers, D. L. Cox, and J. W. Wilkins

Laboratory of Atomic and Solid State Physics, Cornell University, Ithaca, New York 14853

(Received 12 October 1984)

A unified view of the mixed-valence system of Ce impurities in a metal results from a comprehensive calculation of its properties. The peak position T_0 of the Kondo resonance in the photoemission spectrum sets the scale for the universal functions describing the specific heat, susceptibility, resistivity, thermopower, thermal conductivity, and neutron-scattering function. Deviations from universality arise when T_0 becomes comparable to the hybridization width Γ or the spin-orbit splitting Δ .

PACS numbers: 75.20.Hr, 72.15.Qm, 76.30.Kg, 79.60.Cn

We report here the results of systematic calculations, using a single method, for an orbitally degenerate model of magnetic impurities in a metal. The computed properties of a Ce impurity system include equilibrium (specific heat¹ and susceptibility¹⁻³), transport (resistivity and thermopower), and excitation properties (photoemission⁴ and inverse photoemission, and the linewidth of the quasielastic peak in neutron scattering).³ For a broad range of parameters each property (except photoemission) is a universal function of the temperature scaled by a characteristic temperature T_0 which can be deduced from a narrow, many-body "Kondo resonance" in the photoemission curve.

The immediate relevance of the calculations is to provide a comprehensive solution to the properties of the magnetic impurity Ce (or Yb). Particularly striking is the fact that the universal functions are insensitive to the relative occupancy $n_f(0)$ of the Ce 4*f* level

from the Kondo limit ($n_f = 1$) into the mixed-valence regime ($n_f = 0.7$). In addition the calculated resistivity agrees with that measured for Ce in LaB₆, for which data for four temperature decades are available.

Less clear is the relevance of the calculations to rare-earth (and actinide) transition-metal alloys and compounds, that is, to mixed-valence materials. That single-impurity effects may dominate some properties, such as the susceptibility or specific heat, is suggested by calculations showing that the interactions between rare-earth ions may be smaller than single-site terms in the mixed-valent regime by an inverse factor of orbital degeneracy.⁵ Unfortunately, these arguments do not seem helpful in explaining the collective properties (such as de Haas-van Alphen or phase transitions) or the transport properties, especially for the burgeoning area of heavy-fermion materials.⁶ Nonetheless the results we report here must surely be included in understanding these concentrated systems.

TABLE I. Parameter values and zero-temperature properties for the Ce impurity with $D = 3$ eV. For the first four data sets, $N_{\text{grd}} = 6$ and $N_{\text{ex}} = 0$; for the last two sets, $N_{\text{grd}} = 6$ and $N_{\text{ex}} = 8$, with $\Delta/D = 0.07$. T_0 is defined as the peak position of the central Kondo resonance in $\rho_{4f}(\omega)$ as $T \rightarrow 0$; $n_f(0)$ and $\tilde{\chi}(0) = 3\chi(0)/\mu_{5/2}^2 N(0)$ [$\mu_{5/2}$ is the $j = \frac{5}{2}$ effective moment; $N(0)$ is the conduction-band density of states at the Fermi level] are extrapolations of our low- T calculations; $\tilde{\gamma}(0) = 3/\pi^2 k_B^2 N(0) \lim_{T \rightarrow 0} [C_V(T)/T]$ is estimated by a Fermi-liquid expression (Ref. 8) for the enhancement in the density of states. Symmetry arguments predict that $\tilde{\chi}(0)/\tilde{\gamma}(0) = N_{\text{grd}}/(N_{\text{grd}} - 1)$; the agreement is good for $n_f(0) \geq 0.86$. We note that for the first five runs,

$$N_{\text{grd}} N(0) \tilde{\gamma} T_0 / (N_{\text{grd}} - 1) = 0.91 \approx e^{-1/6} / \Gamma(1 + \frac{1}{6}),$$

a factor found in systematic larger- N perturbation theory (Ref. 9).

Data set	Γ/D	$10^4 k_B T_0/D$	$n_f(0)$	$\tilde{\gamma}(0)$	$\tilde{\chi}(0)/\tilde{\gamma}(0)$
Circle	0.05	5	0.97	4980	1.20
Square	0.075	53	0.92	452	1.19
Filled circle	0.10	180	0.86	135	1.20
Asterisk	0.20	1100	0.71	20	1.18
Cross	0.035	9	0.96	2730	1.18
Triangle	0.05	150	0.86	162	1.12

The essential ingredients of the Ce impurity model that we solve are as follows⁷: (i) A structureless conduction band described by a Lorentzian density of states centered at the Fermi level with half-width D (~ 3 eV, say); the density of states at the Fermi level $N(0) = (\pi D)^{-1}$. (ii) An orbitally degenerate f level whose occupancy n_f cannot exceed unity (in the case of Yb the hole occupancy cannot exceed unity). We can include spin-orbit effects by placing a ground level ($j = \frac{5}{2}$) at $\epsilon_{5/2} = \epsilon_f$ with orbital degeneracy $N_{\text{grd}} = 6$ and an excited level ($j = \frac{7}{2}$) at $\epsilon_{7/2} = \epsilon_f + \Delta$ with $N_{\text{ex}} = 8$. For Ce, $\epsilon_f \approx -2$ eV and the spin-orbit interaction $\Delta \approx 0.25$ eV. (iii) The hybridization width of the f level due to the conduction band is Γ (< 0.1 eV). Table I gives the actual parameter values used in the six calculations that we report.

We have adopted a self-consistent perturbation theory developed recently¹⁰ which circumvents the divergences of conventional perturbation theory and allows for the calculation of dynamics. The characteristic temperature T_0 which emerges from our calculations is proportional to the Kondo temperature T_K , the temperature scale for renormalized high-temperature expansions.¹¹ If we define a dimensionless coupling constant $g = \Gamma/\pi|\epsilon_f|$, then a good estimate¹² of T_0 is

$$T_0 = D [1 + D/(T_0 + \Delta)]^{N_{\text{ex}}/N_{\text{grd}}} \times g^{1/N_{\text{grd}}} \exp(-1/N_{\text{grd}}g). \quad (1)$$

The most important feature of (1) is that increasing Γ or N_{grd} dramatically increases T_0 . If T_0 is comparable to the hybridization width Γ , the bandwidth D , or the spin-orbit splitting Δ , we expect deviations from universal behavior as a function of T/T_0 .

Figure 1 shows $\rho_{4f}(\omega)$ for Ce and Yb. The curve in Fig. 1(a) for γ -Ce at room temperature illustrates all the main features⁴: (i) The broad ($\sim 14\Gamma$) feature near ϵ_f (~ -2 eV) contains most of the $4f$ weight and is insensitive to temperature. (ii) The central "Kondo resonance" has a peak position which at low temperature would agree with T_0 given by Eq. (1) to within a few percent. (iii) The sidebands at $T_0 \pm \Delta$ (first pointed out by Gunnarsson and Schönhammer⁴ for Ce compounds) are due to the virtual exchange between multiplets; the sideband below the Fermi level is broadened on the scale of Γ and the one above on the scale of T_0 . Discussion of α -Ce is given in the figure caption in order to stress here the analogies between Ce and Yb.

The entire discussion for the electron spectra of Ce can be repeated for the hole spectra of Yb by inversion of the energy scale,¹³ provided that $4f^{13}$ is stable ($\epsilon_f > 0$). Thus (i) the broadened peak near ϵ_f for f^{13} lies at positive energy, (ii) the Kondo resonance lies below the Fermi level, and (iii) the sideband at

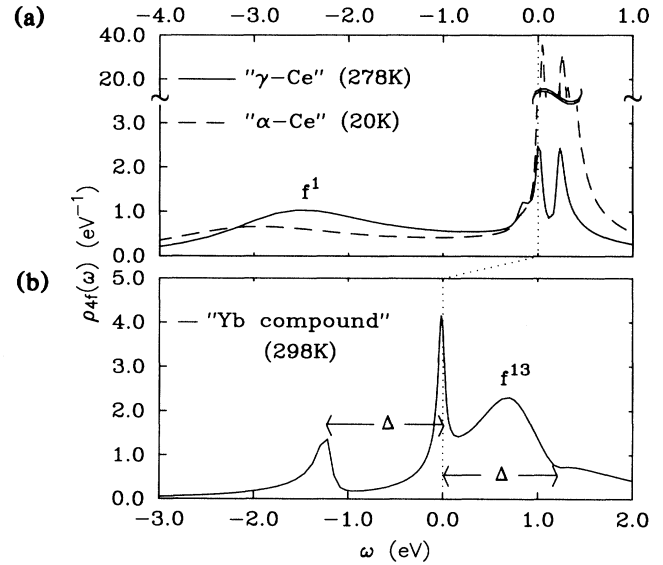


FIG. 1. Calculated $4f$ density of states of our model for Ce and Yb as a function of energy relative to the Fermi level. For $\omega < 0$, $\rho_{4f}(\omega)$ is the electron removal (photoemission) spectrum, and for $\omega > 0$, the electron addition (inverse photoemission) spectrum. (a) The central $j = \frac{5}{2}$ Kondo resonance (near energy $k_B T_0$) has weight $\approx 6[1 - n_f(T)]$. The only difference between γ -Ce (cross in Table I) and smaller volume α -Ce (triangle) is that the latter, calculated at low temperature, has a hybridization width $\sim 30\%$ larger. This single change (i) reduces n_f from 0.96 (γ -Ce) to 0.86 (α -Ce) and (ii) suppresses the low-temperature susceptibility and specific heat by a factor of 15, while radically increasing $\rho_{4f}(\omega)$ above the Fermi surface. The increase in Γ also washes out the lower sideband at $T_0 - \Delta$. (b) The $\rho_{4f}(\omega)$ calculation for Yb assumes ϵ_f for f^{13} at 1.0 eV with $\Gamma = 0.054$ eV and $\Delta = 1.2$ eV.

$T_0 - \Delta$ is broadened on the scale of T_0 . Because of interference with the peak at ϵ_f , the upper spin-orbit feature is an antiresonance. The large spin-orbit interaction ($\Delta \sim 1.2$ eV) would permit ready resolution of the lower sideband.

Figure 2 shows the calculated static magnetic susceptibility $[\chi(T)]$ and quasielastic neutron-scattering linewidth $[\Gamma_Q(T)]$. Γ_Q is here defined as the peak position in the dynamical susceptibility $\chi''(\omega, T)$. The good agreement of $\chi(T)$ with exact Bethe Ansatz results¹ confirms the validity of the calculational method. $\chi(T)/\chi(0)$ is a universal function of T/T_0 , even for $n_f(0)$ as low as 0.86. In general the deviations from the universal curve for values of T_0/Γ (T_0/Δ) greater than one-half (one-tenth) arise when the contributions of the broad ϵ_f peak and the sidebands become important. Γ_Q/T_0 also shows universal behavior; the linewidth is constant for $T < T_0$ and roughly proportional to $T^{1/2}$ for $T > T_0$.

Figure 3 displays the first calculation of the resistivi-

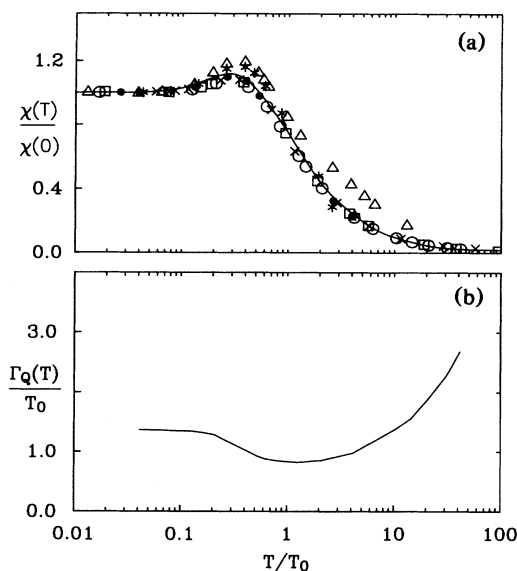


FIG. 2. (a) Static susceptibility and (b) quasielastic linewidth of Ce impurity as a function of T/T_0 for various parameter choices. See Table I for the identification of the various runs; T_0 is the position of the low-temperature Kondo resonance in $\rho_{4f}(\omega)$ (cf. Fig. 1). (a) The magnetic susceptibility was calculated by a Kubo formula. Increasing the hybridization width Γ or including spin-orbit effects produces deviations from the exact Bethe Ansatz result (Ref. 1) (solid line) for $j = \frac{7}{2}$ and $n_f = 1$ (note that because of a different density of states a scale shift in $\ln T$ was required to align the peak in Ref. 1 with our results). The run with $T_0/\Delta \approx 0.2$ corresponds more nearly to the universal curve of Ref. 1 with an effective degeneracy of the order of 8. (b) The neutron quasielastic linewidth Γ_Q was estimated as the peak position of the dynamical susceptibility $\chi''(\omega, T)$.

ty (accurate over the full temperature range) and the thermopower. These, along with the thermal conductivity, have been computed with use of standard transport integrals and the proportionality between the conduction electron scattering rate $\tau^{-1}(\omega)$ and $\rho_{4f}(\omega)$.¹⁴ See the figure caption for details of the universality.

We now turn to the experimental confirmation of these calculations. The most extensive previous comparisons have occurred for the photoemission and inverse-photoemission spectra.⁴ For individual compounds good fits have been obtained for the susceptibility and specific heat.¹⁵ An especially favorable system¹⁶ for comparison with the experiment is $(La, Ce)B_6$. The Ce crystal-field ground state in this system is believed to be a Γ_8 quartet. A good fit to the measured resistivity is nevertheless possible under the assumption that $N_{\text{grd}} = 6$ (see Fig. 3). Susceptibility,¹ specific heat,¹ and thermopower are more sensitive to ground-state degeneracy, and a quantitative comparison requires that $N_{\text{grd}} = 4$.¹⁷ Finally, preliminary stud-

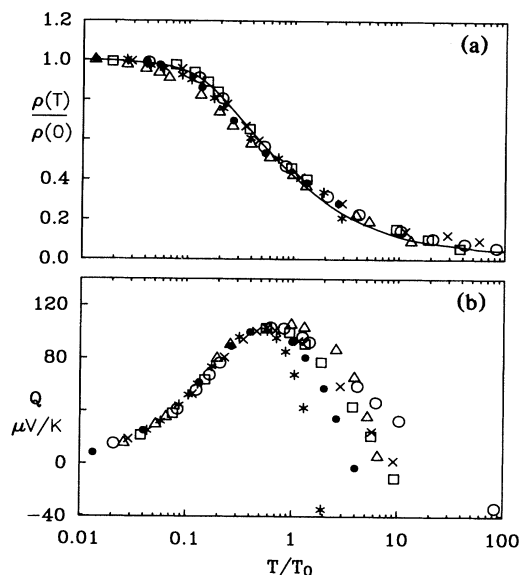


FIG. 3. (a) Resistivity and (b) thermopower of Ce impurity as a function of T/T_0 . Symbols are the same as in Fig. 2. (a) The resistivity, scaled with respect to its zero-temperature value, exhibits universal behavior. In particular, for $T \ll T_0$, $\rho(T)/\rho(0) = 1 - 5(T/T_0)^2$ and for $T \sim T_0$, $\rho(T)/\rho(0) = 0.4 - \ln(T/T_0)$. The solid curve (Ref. 16) is for dilute Ce in LaB_6 . A value of $T_0 = 1.6$ K was deduced from the first decade of the data. (b) The thermopower shows the largest deviations from universality. An extra power of energy in the relevant transport integral causes Q to sample the ϵ_f peak and sidebands at lower temperature; the deviations in the thermal resistivity occur at even lower temperatures.

ies suggest that neutron-scattering data for $CePd_3$, $CeSn_3$, and $YbCuAl$ are consistent with the linewidth calculations reported in Fig. 2.^{18,19} In particular, for low- T_0 ("Kondo") compounds, the rise in $\Gamma_Q(T)$ above T_0 has been measured; for high- T_0 ("mixed-valent") compounds, only the constant piece below T_0 has been seen.

This work was supported by the National Science Foundation under Grant No DMR-8314764; one of us (N.E.B.) acknowledges receipt of a National Science Foundation predoctoral fellowship. We are grateful for the hospitality of the IBM Thomas J. Watson Research Center where some of this work was done.

¹V. T. Rajan, Phys. Rev. Lett. **51**, 308 (1983).

²F. C. Zhang and T. K. Lee, Phys. Rev. B **30**, 1556 (1984).

³H. Kojima, Y. Kuramoto, and M. Tachiki, Z. Phys. B **54**, 293 (1984). We note that these authors obtained linewidth results above the Kondo temperature similar to ours.

⁴O. Gunnarsson and K. Schönhammer, Phys. Rev. Lett.

50, 604 (1983), and Phys. Rev. B **28**, 4315 (1983).

⁵P. Coleman, Phys. Rev. B **28**, 5255 (1983).

⁶G. R. Stewart, Rev. Mod. Phys. **56**, 755 (1984).

⁷P. W. Anderson, Phys. Rev. **124**, 41 (1961). Anderson first suggested a $1/\text{degeneracy}$ expansion for the mixed-valent problem in *Valence Fluctuations in Solids*, edited by L. M. Falicov *et al.* (North-Holland, Amsterdam, 1981), p. 451.

⁸A. Yoshimori, Prog. Theor. Phys. **55**, 67 (1976); P. Noziers and A. Blandin, J. Phys. (Paris) **41**, 193 (1980).

⁹J. W. Rasul and A. C. Hewson, J. Phys. C **17**, 3337 (1984).

¹⁰P. Coleman, Phys. Rev. B **29**, 3035 (1984); H. Keiter and G. Czycholl, J. Magn. Magn. Mater. **31**, 477 (1983); Y. Kuramoto, Z. Phys. B **53**, 37 (1983); F. C. Zhang and T. K. Lee, Phys. Rev. B **28**, 33 (1983). The anomalies known to arise in this method for $T=0$ were not observed in our calculations. Zero-temperature results were computed by extrapolations from finite T .

¹¹N. Andrei, K. Furuya, and J. H. Lowenstein, Rev. Mod. Phys. **55**, 331 (1983).

¹²That T_0 was proportional to $\exp(-1/N_{\text{grd}}g)$ was first pointed out by B. Coqblin and J. R. Schrieffer, Phys. Rev. **185**, 847 (1969). The multiplicative prefactor was derived in Ref. 4 and by K. Yamada, K. Yosida, and K. Hanzawa, Prog. Theor. Phys. **71**, 450 (1984).

¹³B. Jones, private communication.

¹⁴D. C. Langreth, Phys. Rev. **150**, 516 (1966).

¹⁵V. T. Rajan, J. H. Lowenstein, and N. Andrei, Phys. Rev. Lett. **49**, 497 (1982).

¹⁶K. Winzer, Solid State Commun. **16**, 521 (1975) (data run from 40 mK to 300 K).

¹⁷H. J. Ernst, H. Gruhl, T. Krug, and K. Winzer, in *Proceedings of the Seventeenth International Conference on Low-Temperature Physics*, edited by U. Eckern, A. Schmid, W. Weber, and H. Wühl (North-Holland, Amsterdam, 1984), p. 137.

¹⁸CePd₃, CeSn₃: E. Holland-Moritz *et al.*, Phys. Rev. B **25**, 7482 (1982); YbCuAl: W. C. M. Mattens *et al.*, J. Magn. Magn. Mater. **15-18**, 973 (1980).

¹⁹D. L. Cox, N. E. Bickers, and J. W. Wilkins, to be published.